論文 / 著書情報
Article / Book Information

Title	Fatigue strength of steel–aluminum alloy dissimilar lap joints fabricated by dimple spot welding for automotive application
Authors	Motoki Sakaguchi, Yu Kurokawa, Fuminori Nakamura, Toru Hashimura
Citation	Fatigue & Fracture of Engineering Materials & Structures, Vol. 47, Issue 3, pp. 939-951
Pub. date	2024, 1
DOI	https://doi.org/10.1111/ffe.14227
Creative Commons	Information is in the article.

Received: 25 August 2023 | Revised: 21 November 2023 | Accepted: 10 December 2023

DOI: 10.1111/ffe.14227

ORIGINAL ARTICLE

FFEMS Fatigue & Fracture of Engineering Materials & Structures WILEY

Fatigue strength of steel–aluminum alloy dissimilar lap joints fabricated by dimple spot welding for automotive application

Motoki Sakaguchi[1] | **Yu Kurokawa**[1] | **Fuminori Nakamura**[1] | **Toru Hashimura**[2]

[1]Department of Mechanical Engineering, Tokyo Institute of Technology, Tokyo, Japan

[2]Kobe Steel, Ltd., Technical Development Group, Kobe, Japan

Correspondence
Motoki Sakaguchi, Department of Mechanical Engineering, Tokyo Institute of Technology, O-okayama 2-12-1, Meguro-ku, Tokyo, 152-8552, Japan.
Email: sakaguchi.m.ac@m.titech.ac.jp

Abstract

Recently, a new dissimilar mechanical joining method, dimple spot welding (DSW), has been developed for joining steel sheets and aluminum alloys. In this study, tensile shear tests and fatigue tests were conducted on four types of dissimilar lap joints, with two types of steel sheets and two types of Al alloys joined by DSW. Both the tensile shear strength and fatigue strength of DSW joints were found equal to or greater than those of a self-piercing riveting (SPR) joint. In all four types of DSW joints, fatigue cracks were initiated from the Al alloy and were associated with fretting induced by repeated contact and friction. A finite element analysis showed that the tangential stress was mainly governed by the friction coefficient and also affected by the steel sheet strength. Higher-strength steel led to lower tangential stress, resulting in a longer fatigue life for the DSW joint.

KEYWORDS

aluminum alloy, dimple spot welding, finite element analysis, fretting fatigue, mechanical joining, multimaterialization, steel sheet

Highlights

- A dimple spot welding (DSW) is developed for joining steel sheets and aluminum alloys.
- Tensile shear tests and fatigue tests are conducted on DSW joints and SPR joint.
- DSW joints shows greater tensile shear strength and longer fatigue lives than SPR joint.
- Fatigue cracks in DSW joints were initiated associated with fretting.

1 | INTRODUCTION

To reduce energy consumption for halting global warming, there is a demand for development of car bodies that both improve fuel economy and ensure collision safety in the automotive industry. High-strength steel sheets have been widely applied to car bodies to reduce weight by reducing the sheet thickness and improve collision safety through strengthening their intrinsic mechanical properties.[1] Nevertheless, there is a limit to weight reduction by reducing the thickness of steel sheets. Lightweight materials, including aluminum alloys, magnesium alloys, and carbon fiber-reinforced plastics (CFRP), are also being used in car bodies. Recently, multimaterialization has been attracting attention.[2] This involves fabricating car bodies by combining lightweight materials with high-strength steel sheets. Particularly, aluminum alloys are being applied to steel car body structures[1,2] which is expected to yield an excellent dissimilar joining method for high-strength steel and aluminum alloys.

Welding is the most widely used joining method in automotive manufacturing, and various welding techniques have been applied to the car body.[1,2] Most joining methods for car bodies involve resistance spot welding. The effects of welding time and current on tensile and fatigue strength have been investigated to examine the mechanical properties of spot-welded joining of high-strength steel plates[3] and the strain distribution in the joint has also been investigated by digital image correlation.[4] Resistance spot welding between steel and aluminum alloys is accompanied by big problems relating to poor welds due to voids and defects inside the nugget as well as to the degradation associated with formation of brittle intermetallic compounds at the welding interface.[2] Hence, various joining methods such as self-piercing riveting (SPR), clinching, spot friction welding, and ultrasonic spot welding have been applied to join dissimilar materials in multi-material car bodies.[5,6] SPR is a joining method where the metal sheets are fastened by mechanical interlocking.[7] A rivet is punched into two metal sheets supported by a die, and then a mechanical interlock is made between the rivet and the two sheets.[7] Tensile shear tests and fatigue tests conducted on the SPR joints of various metal plates have shown that the strength of SPR joints is comparable to that of spot-welded joints.[8–10] However, these mechanical joints require incorporating dedicated joining equipment into the car body production line, which is very costly. To develop a method that fabricates a high-strength dissimilar joint using existing welding equipment, Hashimura et al.[11] have developed a new dissimilar mechanical joining method, dimple spot welding (DSW), for joining steel sheets and aluminum alloys.

The DSW joining process[11] is shown schematically in Figure 1. First, a dimple is pressed into the steel sheet, while a hole is drilled into the aluminum alloy plate. Second, an additional steel sheet called a backing plate is prepared. The Al alloy plate is sandwiched by the steel sheet and backing plate, and the dimple of the steel plate is brought into contact with the backing plate through the hole of the Al alloy plate. The contact areas of the steel plate and backing plate are welded by resistance spot welding to firmly sandwich the Al alloy plate, and then a dissimilar joint of the steel sheet and Al-alloy plate can be fabricated. The advantage of DSW is using existing equipment for resistance spot welding that is widely used in actual production lines for car bodies, thus the joining can be achieved without modification. Hashimura et al. fabricated DSW dissimilar-material joints with the hole diameter of the Al alloy plate and the dimple depth of the steel plate as changing variables and conducted tensile shear tests and cross-tension tests.[11] They found that the static strength of DSW joints is equivalent or superior to that of joints produced through existing methods such as SPR and that the tensile shear strength and cross-tension strength depend on the hole diameter and dimple depth.[11] Fatigue strength under cyclic loading is also important when considering a structural material for practical application to a car body. In addition, the influences of the base material and combination of steel sheet and Al alloy also need to be considered.

The purpose of this study is to clarify fatigue properties of dissimilar steel/aluminum alloy joints fabricated by DSW. Four types of DSW lap joints were prepared by changing combinations of steel sheets and Al alloys, involving two types of steel sheets and two types of Al alloys. Tensile shear tests and fatigue tests were performed at room temperature. The same tests were performed on an SPR joint for comparison. Tensile shear tests and fatigue tests have already been conducted in the previous study.[12] This study combines the previous experimental data with the results of additional fatigue tests, and the fatigue failure of DSW joints is examined considering the stress at the contact surface via elastic plastic analysis using the finite element (FE) method.

2 | MATERIALS AND METHODS

2.1 | Dissimilar joining using DSW

Four types of DSW specimens were prepared by joining two types of Al alloys and two types of steel sheets by DSW. The two Al alloys were 6000 series (A6N01-T5) and 7000 series (A7003-T5), and the two steel sheets were tensile strength 590 MPa class (SPC590) and 980 MPa class

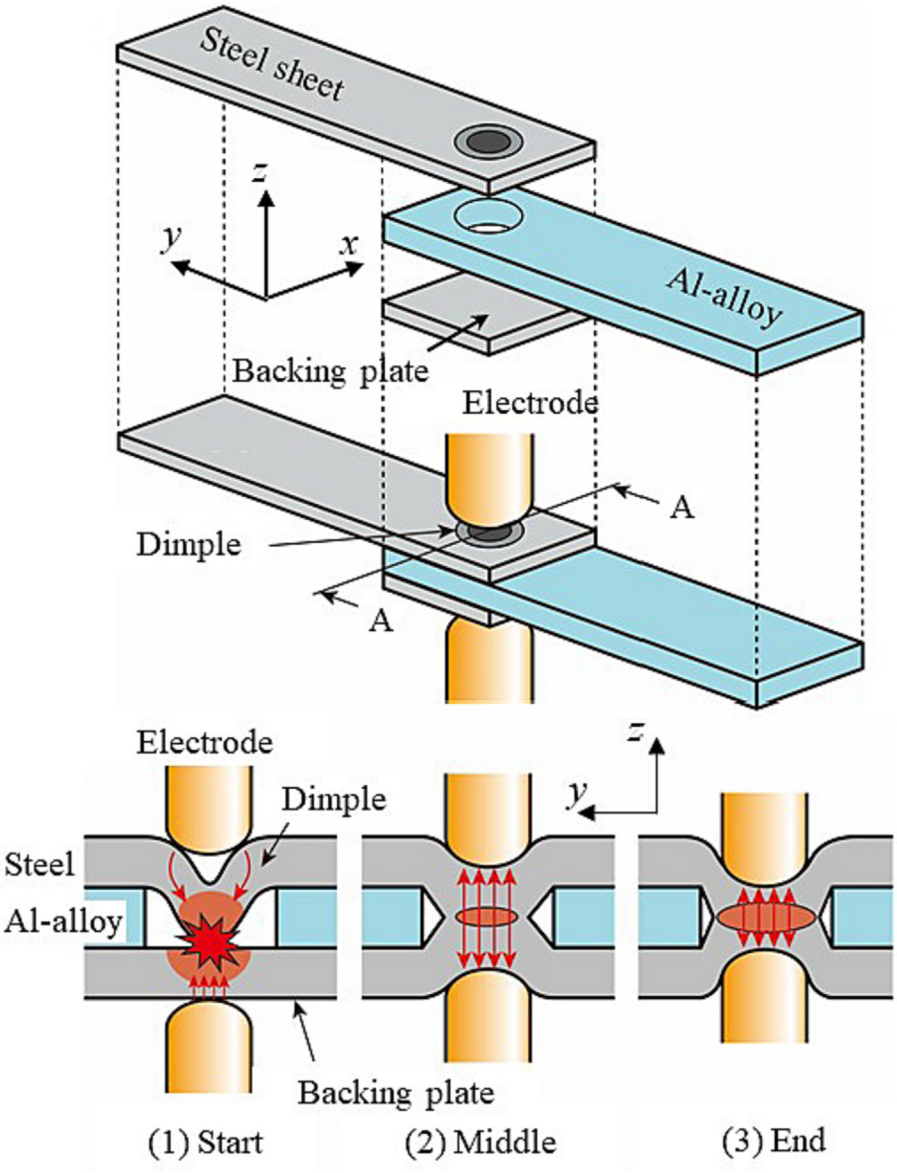

FIGURE 1 Illustrations of joining through dimple spot welding (DSW). [Colour figure can be viewed at wileyonlinelibrary.com]

(SPC980). Table 1 shows the combination of steels and Al alloys used for the four types of DSW specimens: DSW-1, DSW-2, DSW-3, and DSW-4. For comparison, a reference specimen was prepared by joining SPC980 and A7003-T5 by SPR. The combination of base materials in the SPR specimen was the same as that of DSW-4. The stress–strain relationships of all base materials in the uniaxial tensile tests are shown in Figure 2. Table 2 summarizes the tensile strength, yield stress and elongation. Figure 3 shows the geometries of the (A) DSW and (B) SPR specimens. The gray and blue areas in the figure indicate the steel and Al alloy, respectively. The dimple depth of the steel sheet used for the DSW specimen was 2.0 mm, and the hole diameter of the Al alloy plate was 10.5 mm. The interlock of the SPR specimens was 0.5 mm. In this study, the *xyz* axes are used to represent the DSW specimen directions shown in Figure 1. The *x*, *y*, and *z* axes correspond to the specimen width, direction of uniaxial loading, and specimen thickness, respectively.

TABLE 1 Steel sheets and aluminum alloys used in DSW and SPR specimens.

Specimen	Aluminum alloy	Steel sheet
DSW-1	A6N01	SPC590
DSW-2	A7003	SPC590
DSW-3	A6N01	SPC980
DSW-4	A7003	SPC980
SPR	A7003	SPC980

Abbreviations: DSW, dimple spot welding; SPR, self-piercing riveting.

A resistance spot welding machine, set up according to a report of Hashimura,[11] was used for DSW joining. A chromium copper DR electrode was used as the welding

electrode. The welding was performed at a constant applied load of 4.5 kN for 10 cycles at 8.5 kA/60 Hz, followed by 10 cycles at 10.5 kA and 10 cycles at 11.5 kA. Figure 4 shows a cross-section of the DSW-2 specimen after joining. The hole of the Al alloy plate is not completely filled in by the steel plate and bucking plate; hence, a gap of approximately 1 mm in width is generated between the steel sheet and Al alloy.

2.2 | Tensile shear test

Tensile shear tests were performed on DSW and SPR specimens using a screw tensile testing machine. An Al alloy tab was bonded to the grip sections to suppress bending deformation during the test. The geometries of tab are illustrated in Figure 3. The test was conducted under displacement control, with a displacement rate of 5 mm/min.

2.3 | Fatigue test

Fatigue tests were conducted at room temperature using the same specimens as in the tensile shear test. An electro-hydraulic fatigue testing machine was used for the tests. The tab was attached to the specimen at the same position as in the tensile shear test. The test was conducted under load control with a sinusoidal frequency of 10 Hz. The load amplitude was set from 0.90 to 3.60 kN, and the load ratio was 0.1.

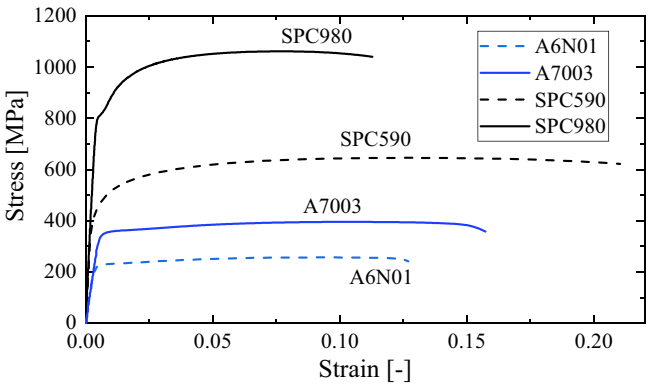

FIGURE 2 Stress–strain relationships of two types of Al alloys and two types of steel sheets. [Colour figure can be viewed at wileyonlinelibrary.com]

3 | RESULTS

3.1 | Tensile shear test results

Figure 5 shows pictures of the DSW and SPR specimens after the tensile shear test. Illustrations of the cross-section are also shown. In the SPR specimen (Figure 5A), the rivet was pulled out from the Al alloy plate, and then the steel sheet and Al alloy were separated. In the cases of DSW-1 and DSW-3, where the Al alloy strength was lower, the Al alloy plate failed owing to stress concentration at the circular hole(Figure 5B). However, in DSW-2 and DSW-4, where the strength of the Al alloy plate is higher, tensile fracture occurred at the weld nugget of the steel sheet (Figure 5C).

First, the tensile shear strengths of the DSW-4 and SPR specimens, which are made of the same base metals, are compared. Because of the difference in joint dimensions, it is not appropriate to evaluate the strength by directly comparing the loads applied to the specimens. For simplicity, the tensile shear strength is compared by dividing the applied load by the area of the joint: for DSW-4, the load is divided by the weld area (23.8 mm^2); for SPR, the load is divided by the cross-sectional area of the rivet shaft (22.9 mm^2). Figure 6 plots these values on the vertical axis as a function of the displacement on the horizontal axis. At the beginning of the test, the load–displacement relationship of DSW-4 has a smaller slope than that of the SPR specimen. This might be because the early deformation of the DSW specimen is accompanied by the penetration of the Al alloy plate into the gap between the steel and Al alloy as shown in Figure 4. In DSW-4, the load temporarily decreased when the vertical axis reached 50 N/mm^2 (circled in Figure 6), at which the trapped contact area of the steel and Al alloy was released and slipped. In Figure 6, the maximum values on the vertical axis are 571 N/mm^2 for DSW-4 and 499 N/mm^2 for the SPR specimen. Therefore, the DSW joint has tensile shear strength equal to or greater than that of the SPR joint.

TABLE 2 Mechanical properties of aluminum alloys and steel sheets used in this study.

Material	Tensile strength (MPa)	Yield strength (MPa)	Elongation (%)
A6N01	257	225	9.4
A7003	395	349	10.8
SPC590	590	444	24.8
SPC980	980	813	13.9

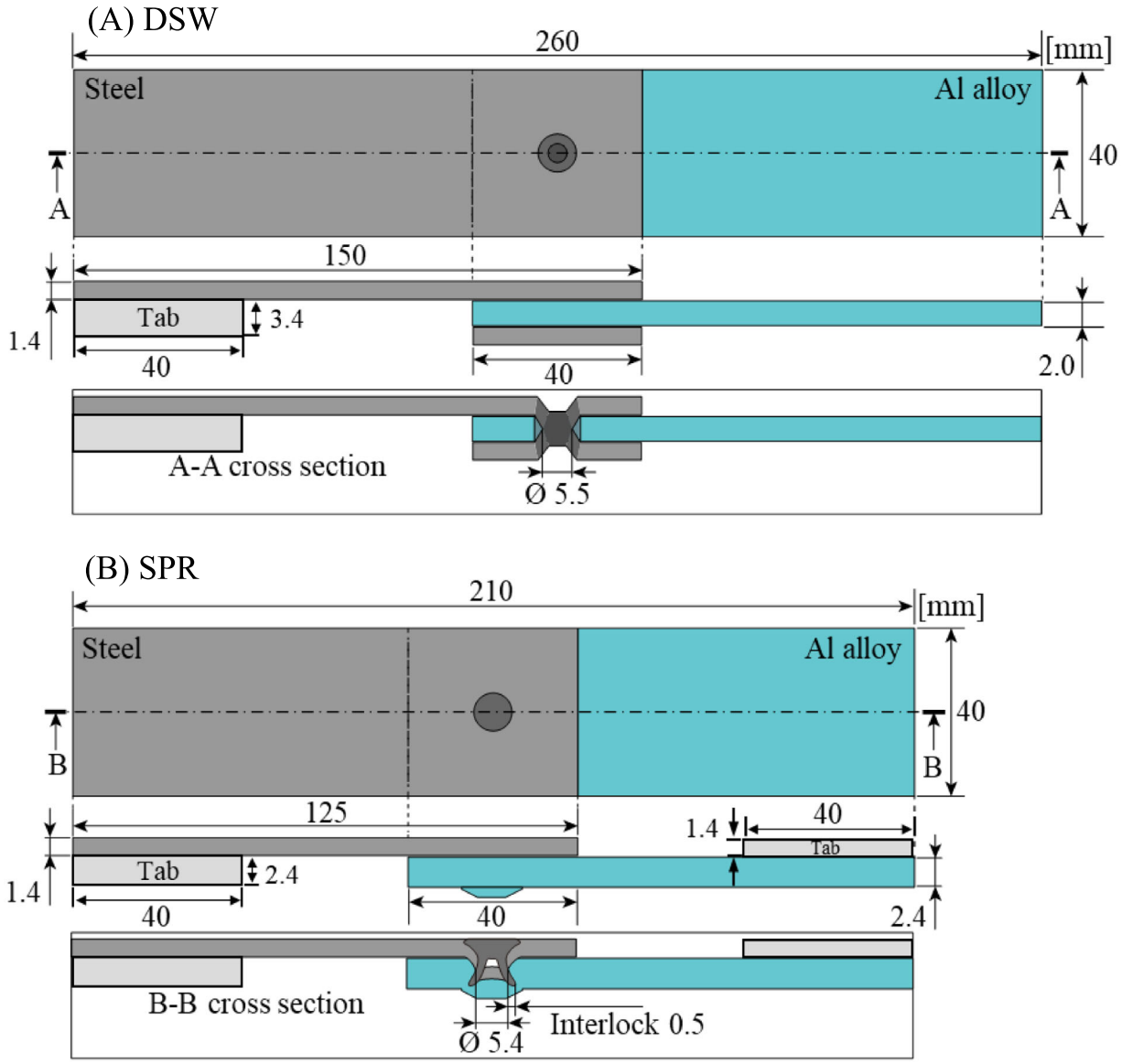

FIGURE 3 Geometries of the dissimilar joint specimens used in this study. (A) DSW and (B) SPR specimens. DSW, dimple spot welding; SPR, self-piercing riveting. [Colour figure can be viewed at wileyonlinelibrary.com]

Table 3 summarizes the tensile shear strengths, which are the maximum loads obtained in the tensile shear tests for the four DSW specimens and SPR specimen. DSW-2 and DSW-4, fabricated with the higher-strength Al alloy, have a tensile shear strength of 13.6 kN, which is higher than that of DSW-1 and DSW-3. The higher-strength Al alloy leads to a higher tensile shear strength for the DSW joint, which is not as affected by the steel sheet strength. In summary, DSW-1 and DSW-3, made with the lower-strength Al alloy plate, failed at the center hole of the Al alloy, and their tensile shear strength was lower than that of DSW-2 and DSW-4, which failed at the weld nugget in the steel sheet. This indicates that the strength of the weld nugget in the DSW joint is higher than that of A6N01 but lower than that of A7003.

3.2 | Fatigue test results

3.2.1 | Fatigue life

Figure 7 shows the fatigue lives of the DSW-4 and SPR specimens with the same combination of steel sheet (SPC980) and Al-alloy (A7003). Here, the number of cycles to failure of the DSW-4 and SPR specimens is compared by dividing the load amplitude by the cross-sectional area of the Al alloy plate on the vertical axis. The fatigue life of the DSW specimen is found to be approximately 10 times longer than that of the SPR specimen, indicating that the DSW joint has superior fatigue strength. Two types of failure modes were observed in the SPR specimen: failure at the rivet under higher load

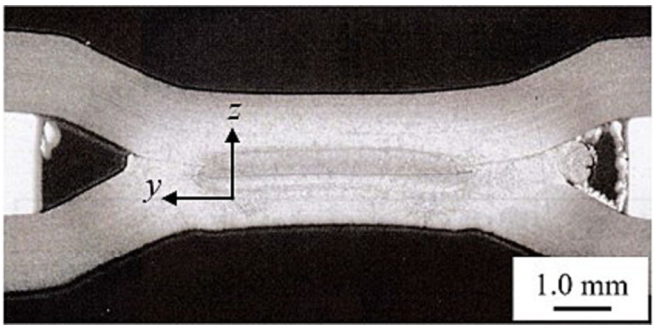

FIGURE 4 Cross-section of DSW-2 specimen. DSW, dimple spot welding.

amplitudes and failure in the Al alloy plate under lower amplitudes. Several studies have also reported that two types of failure modes, rivet failure and base metal failure, are mixed in the fatigue failure of dissimilar SPR joints.[9,10] In contrast, all of the DSW-4 specimens (and the other three specimen types, DSW-1, DSW-2, and DSW-3) were fractured in the Al alloy plate. The failure modes of the DSW specimens are discussed in detail in Section 3.2.2.

The fatigue lives of the four DSW specimen types are compared in Figure 8. Comparing DSW-1 and DSW-2, in which the same steel sheet (SPC590) is used, reveals that the fatigue life of DSW-2 is longer than that of DSW-1. This is simply because the higher-strength Al alloy (A7003) is used in DSW-2 and the intrinsically superior strength of A7003 results in the longer fatigue life of DSW-2. For the same reason, DSW-4 shows a longer fatigue life than DSW-3. However, DSW-3 with higher-strength steel sheet has a longer fatigue life than DSW-1, even though the same Al alloy is used in both and the fatigue failure occurs in this Al alloy plate. The trend is similar for DSW-2 and DSW-4: DSW-4 shows a longer fatigue life than DSW-2. These test results reveal that the fatigue failure in DSW joints occurs in the Al alloy plate, and that while fatigue life is mostly determined by the Al alloy strength, it is also affected by the steel sheet strength. The effect of the steel sheet is related to the fretting fatigue, which is specific to the lap joint as discussed in Section 3.2.2.

3.2.2 | Fracture process during the cyclic loading in DSW joint

In all the fatigue tests of DSW specimens, fatigue failure occurred in Al alloys. Figure 9 shows a typical feature of the side and fracture surfaces of the Al alloy plate. This figure shows pictures of the DSW-1 specimen subjected to a load amplitude of 2.25 kN. Figure 9A shows that fatigue cracks were initiated at the lower right (4 o'clock position) and lower left (8 o'clock position) of the circular center hole in the Al alloy and then propagated in a direction perpendicular to the applied cyclic loading. Close observation of the 4 o'clock positions shows that the area near the crack initiation is discolored black, which is a feature unique to the fatigue test, not observed in the DSW specimens after the tensile shear test (Figure 5B,C). On the fracture surface at the crack initiation site (Figure 9C), the initiated crack is associated with a black mark, which might be due to the accumulation of oxidized black wear debris. Although the crack initiation process could not be observed in-situ because the Al-alloy surface was hindered by the steel sheet, the crack initiation site can be estimated as being at the center of the radial pattern indicated by the red line in Figure 9C. As revealed in Figure 9B,C, this crack initiation site is not at edge of the hole but approximately 1 mm inside the hole. In fatigue tests of riveted and bolted joints,[10,13] cracks typically originate in the heavy fretting area around the riveted or bolted zone a short distance away from the holes, where black wear debris is often observed. Hence, the black debris observed in Figure 9 is related to the repeated contact, suggesting that fretting occurs in DSW specimens during cyclic loading.

The surface of the Al alloy (Figure 9A) also shows a white discolored area on the top side (12 o'clock position), where contact and friction also occurred during the fatigue test. However, no crack is observed on this top side in Figure 9A. This is attributed to the normal stress distribution along the hole, which will be numerically discussed on the basis of the FE analysis in Section 4.

In the tensile shear test, the tensile fracture occurred at the weld nugget of the steel sheet, but this fracture was not observed in the fatigue test. It is assumed that the stress concentration at the weld nugget was not large enough to cause tensile fracture because the load applied to the specimen in the fatigue test was smaller than that in the tensile shear test. The fatigue failure occurred in the Al alloy plate before the tensile fracture in the steel sheet in the fatigue test on the DSW specimens.

4 | DISCUSSION

There are severe stress gradients at the contact interface due to frictional and tangential loads, which act as a flaw generator leading to premature crack nucleation when compared with plane fatigue situations.[14–16] In this study, fatigue tests were conducted on four types of DSW specimens with different combinations of steel sheets and Al alloys. All specimens were fractured in

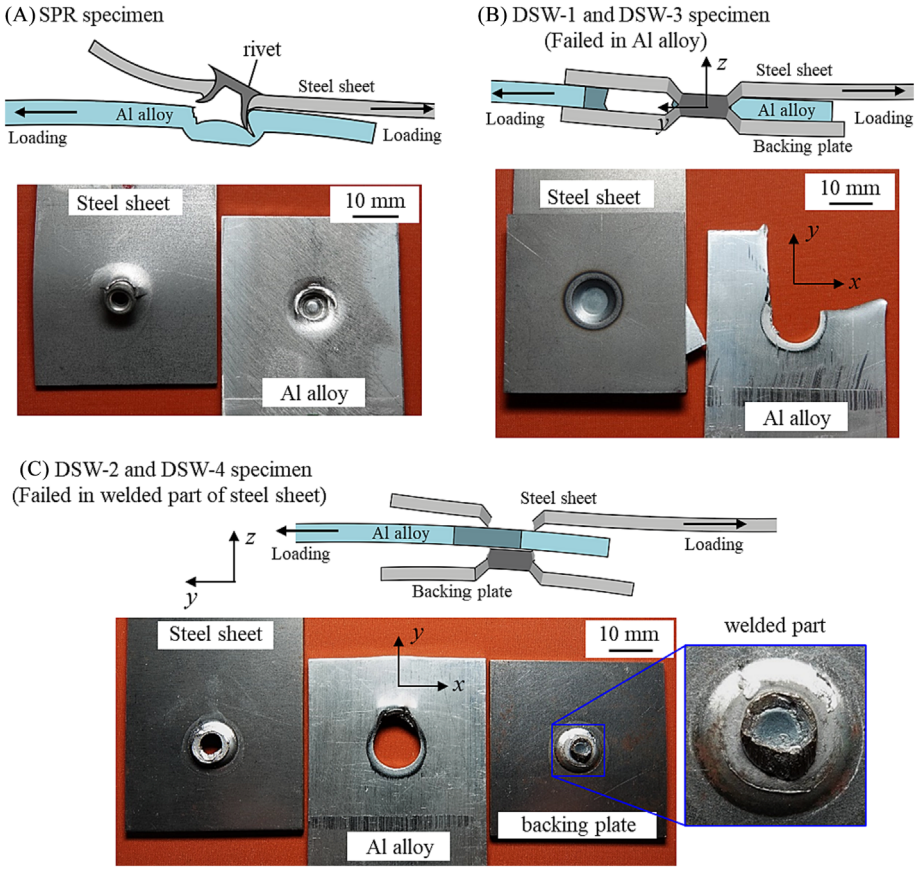

FIGURE 5 Overviews of the tensile shear test specimens. (A) SPR, (B) DSW-1 and 3, and (C) DSW-2 and DSW-4. DSW, dimple spot welding; SPR, self-piercing riveting. [Colour figure can be viewed at wileyonlinelibrary.com]

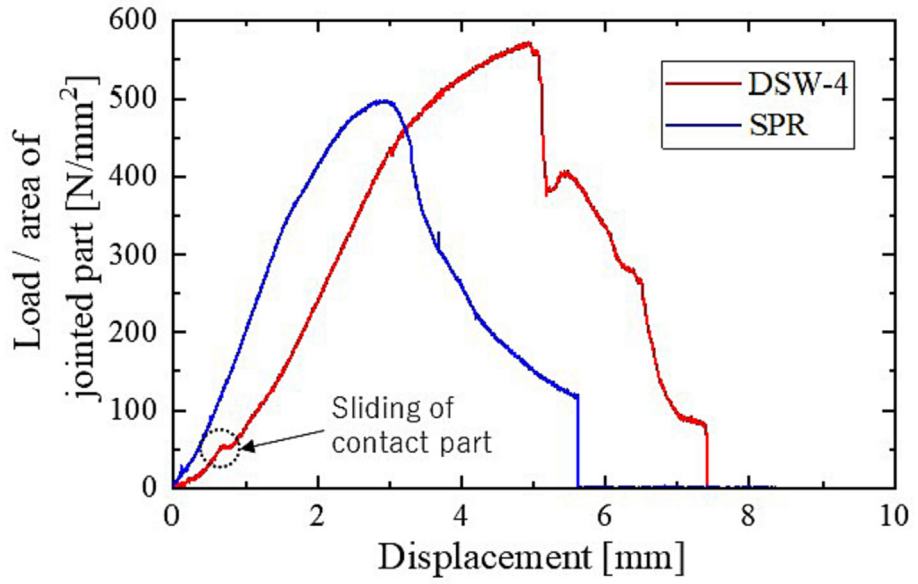

FIGURE 6 Load–displacement curves of DSW-4 and SPR specimens in the tensile shear test. DSW, dimple spot welding; SPR, self-piercing riveting. [Colour figure can be viewed at wileyonlinelibrary.com]

the Al alloy plate, and the fatigue life was found to be affected not only by the strength of Al alloy itself but also by the mechanical properties of the steel sheets. The stress at the contact surface was affected by (1) the mechanical properties of the steel sheets and Al alloys and (2) the friction coefficient, which depended on the combination of base metals. This then affected the accumulation of fatigue damage in the Al alloy plates. In this section, DSW specimens are reproduced by an FE model, and the effects of the combination of base metals on the stress along the contact surface are examined numerically.

4.1 | FE model of the DSW dissimilar joint

FE analysis is conducted using Abaqus/Standard 2017. Figure 10 shows the FE model used in this study. Half of the actual DSW specimen is modeled considering the symmetry along the width direction. The geometry is determined from the cross-sectional picture of the actual joint as seen in Figure 4. An eight-node brick element with reduced integration (C3D8R) was used as the main element, and a six-node wedge element (C3D6) was partially used. The minimum element size near the weld area was approximately 0.05 × 0.05 × 0.1 mm, and the mesh was set so that the element size increased away from the weld area. The mechanical properties of the base metals were set according to the stress–strain relationships under the uniaxial tensile tests shown in Figure 2. The Poisson's ratios of the steel sheets and Al alloys were set to 0.30 and 0.34, respectively. The Mises yield criterion was considered for the yield condition. The friction coefficients in Table 4 were measured for four combinations of base metals. Here, Model-1, Model-2, Model-3, and Model-4 correspond to the actual specimens DSW-1, DSW-2, DSW-3, and DSW-4, respectively, where the measured friction coefficients are used. Model-1′, Model-2′, Model-3′, and Model-4′ are hypothetical models in which only the friction coefficients are changed without changing the other mechanical properties to examine the effect of the friction coefficient.

In the DSW joints, residual stresses are generated when the steel sheets are welded through the hole drilled in the Al alloy plate. Such residual stresses firmly grip the Al alloy plate. In fact, half of the Al alloy plate remained between the steel sheets even after the tensile shear test as seen in Figure 5B. In the FE analysis, the Al alloy plate was simulatively heated to reproduce the

TABLE 3 Tensile shear strengths of four DSW specimens and an SPR specimen.

Specimen	Tensile shear strength (kN)	Tensile shear strength/area of jointed part (N/mm^2)
DSW-1	10.6	445
DSW-2	13.7	576
DSW-3	10.5	441
DSW-4	13.6	571
SPR	11.4	499

Abbreviations: DSW, dimple spot welding; SPR, self-piercing riveting.

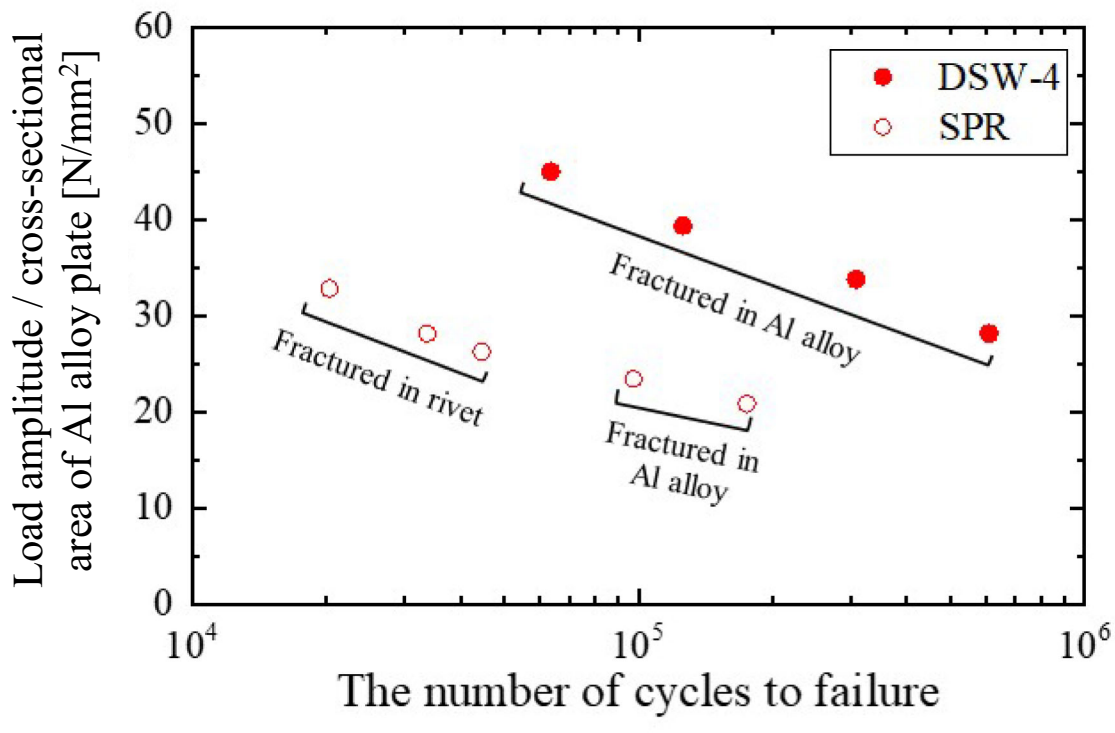

FIGURE 7 Fatigue test results for DSW-4 and SPR specimens. DSW, dimple spot welding; SPR, self-piercing riveting. [Colour figure can be viewed at wileyonlinelibrary.com]

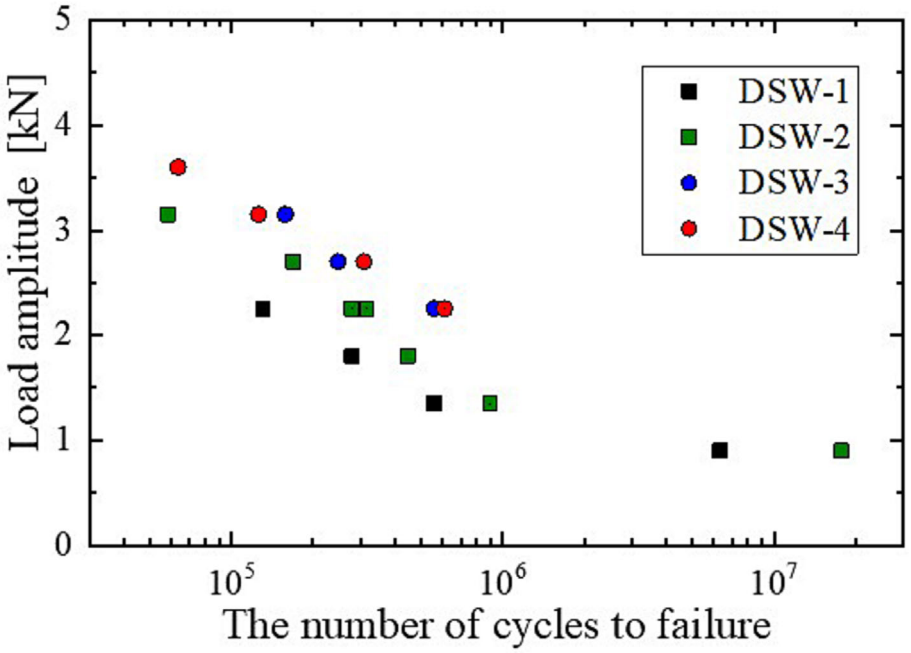

FIGURE 8 Fatigue test results for four DSW specimens. All four specimens were fractured in Al alloy plates. DSW, dimple spot welding. [Colour figure can be viewed at wileyonlinelibrary.com]

compressive residual stress in the Al alloy. Although the residual stress distribution is difficult to reproduce exactly, the load–displacement diagram in Figure 6 for the DSW specimens could be approximately reproduced when the temperature of the Al alloy plate was increased to 400°C for all four joint types.

4.2 | FE analysis results

The stress under a typical frictional contact appears to be highly multiaxial and undergoes nonproportional loading.[14,17] Various parameters have been used to quantitatively describe fatigue damage in complex stress conditions, following critical plane approaches including Fatemi-Socie,[18] Smith-Watson-Topper,[19,20] and others.[21–23] Fretting specific parameters, such as Ruiz parameter[24] and the tangential stress range-compressive stress range diagram,[25] have also been adopted to life prediction under fretting conditions. The optimum parameters seem to vary depending on the combination of materials, the geometry of the contact area, and the level of cyclic loading.[16] The most important parameter in the fretting fatigue is the tangential stress component along the contact surface.[26,27]

Figure 11 shows the distributions of tangential stress σ_T, relative slip range $\Delta\delta$, and maximum principal stress σ_1 along the contact surface of the Al alloy plate. An external load of 5 kN, corresponding to the maximum load during the cyclic loading with load amplitude of 2.25 kN, is applied to Model-1. The tangential stress σ_T, which is an output of *Cshear* in Abaqus/Standard, is induced by the combination of contact pressure and applied stress. Figure 11 shows that higher σ_T is generated at the lower left (8 o'clock position) at a short distance from the hole, at which the relative slip range ($\Delta\delta$) also shows larger value. This position corresponds well to the actual site of crack initiation in the DSW specimen (Figure 9). The crack initiation was caused by the accumulation of fatigue damage due to the repeated contact between the steel sheet and Al alloy at this 8 o'clock position, which resulted in fatigue failure. In Figure 11, σ_T is also high around the top side (12 o'clock position), where a certain level of fatigue damage should be accumulated. Actually, a white discolored area due to the repeated contact and friction was observed on the top side of the DSW specimens as seen in Figure 9A. However, no cracking occurred at this position, unlike the 8 o'clock positions. This is attributed to the distribution of the maximum principal stress σ_1: the σ_1 value around the 8 o'clock position is tensile, whereas that around the 12 o'clock position is compressive. This prevents crack propagation even if a crack is initiated by high tangential stress; therefore, the Al alloy plate never failed from the top side. Actually, no crack is observed around the 12 o'clock position in Figure 9A, although repeated friction also occurred here.

The computed values of σ_T are plotted in Figure 12. The values of σ_T at the nodes along red lines (in the insert) are plotted as functions of the angle from the bottom position (6 o'clock position). Figure 12A shows the results of the lower-strength Al alloy (Model-1 and

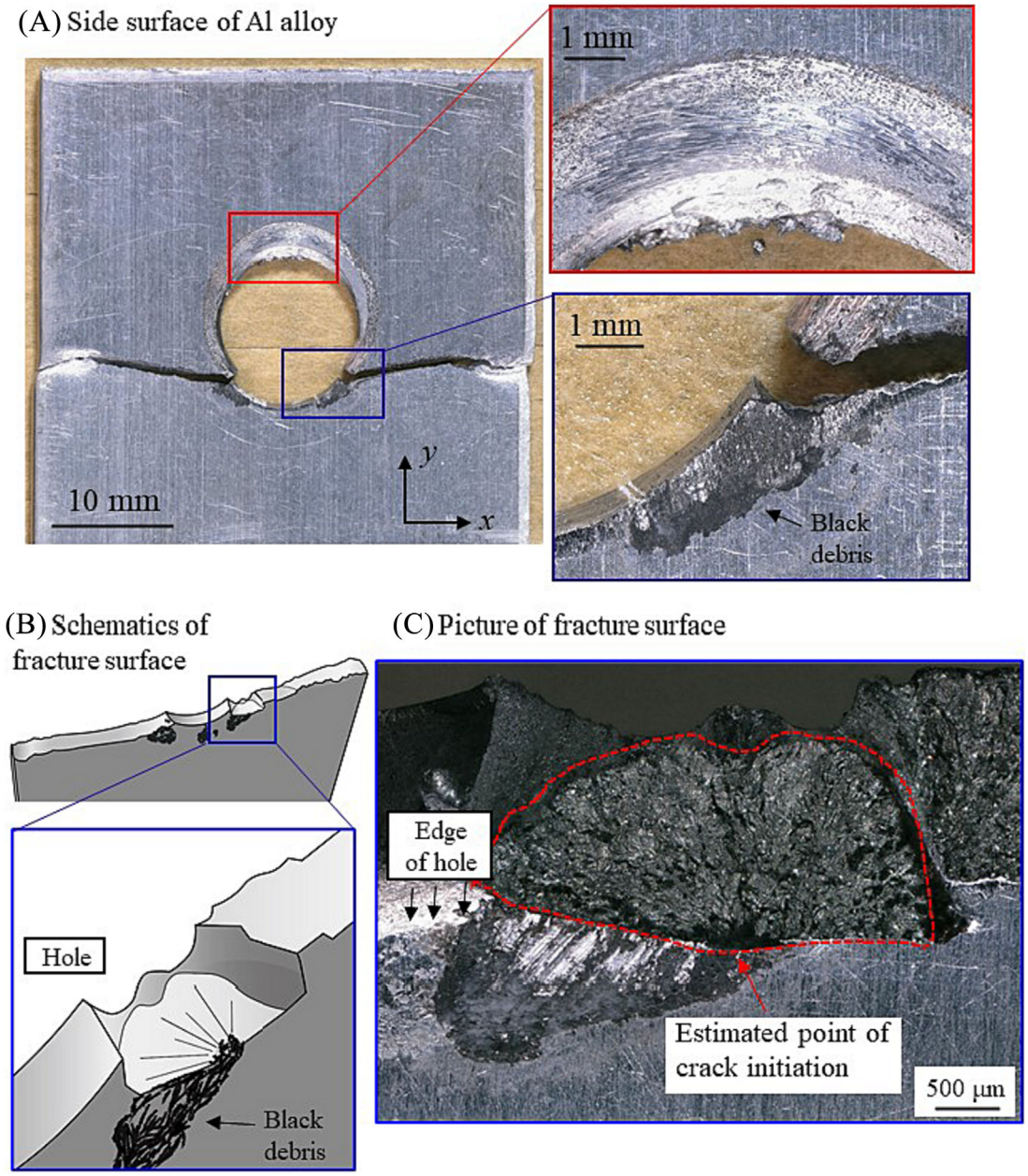

FIGURE 9 The side view and fracture surfaces of Al alloy in DSW-1 specimen (stress amplitude is 2.25 kN). (A) Side surface of Al alloy, (B) illustration of failed, specimen and (C) fracture surface near the crack initiation site. DSW, dimple spot welding. [Colour figure can be viewed at wileyonlinelibrary.com]

Model-3), while Figure 12B shows those of the higher-strength Al alloy (Model-2 and Model-4). The reason why these results are separated in Figure 12 is that the resistance to fatigue damage is different for each Al alloy, so they cannot be directly compared in a single figure. Figure 12A,B shows that the σ_T value for Model-1 and Model-2, in which the Al alloys are joined with the lower-strength steel, are higher than those for Model-3 and Model-4, where the Al alloys are joined with the higher-strength steel. The higher tangential stress leads to higher fatigue damage, resulting in shorter fatigue life. The computed results in Figure 12 are consistent with the fatigue test results in Figure 7.

The steel sheet has two effects on the tangential stress along the contact surface of the Al alloy plate: (1) the mechanical properties of the steel sheet can change the stress at the contact surface and (2) the combination of steel sheets and Al alloys can change the friction coefficient, which affects the tangential stress at the contact surface. Figure 12A,B also shows the resulting values of

σ_T for Model-1′, Model-2′, Model-3′, and Model-4′, for which only the friction coefficient is hypothetically changed. Comparing the cases where the base materials are the same but only the friction coefficient is different (comparing Model-1 with 1′, Model-3 with 3′, Model-2 with 2′, and Model-4 with 4′) reveals that the tangential stress is significantly reduced by the decrease in the friction coefficient. This suggests that the friction coefficient has a more significant effect on the tangential stress in the DSW specimen. However, comparing the four combinations with the same friction coefficient but different steel sheets (comparing Model-1 with 3′, Model-1′ with 3, Model-2 with 4′ and Model-2′ with 4) shows that the specimen with the higher-strength steel has slightly lower tangential stress, suggesting that the resistance of the DSW joint to fretting failure is further increased by the mechanical properties of the steel sheet. The effect of the mechanical properties of the steel sheet is less significant than that of the friction coefficient, but the higher-strength steel sheet has an advantage in improving the fatigue property of the DSW joint.

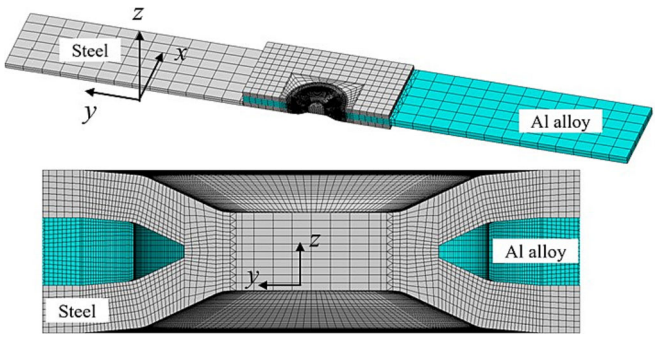

FIGURE 10 Finite element (FE) model of the DSW specimen used in this study. DSW, dimple spot welding. [Colour figure can be viewed at wileyonlinelibrary.com]

TABLE 4 Friction coefficients used in the FE models.

FE model	Frictioncoefficient	Aluminum alloy	Steel
Model-1	0.56	A6N01	SPC590
Model-1′	0.42[a]		
Model-2	0.45	A7003	SPC590
Model-2’	0.38[a]		
Model-3	0.42	A6N01	SPC980
Model-3′	0.56[a]		
Model-4	0.38	A7003	SPC980
Model-4’	0.45[a]		

Abbreviation: FE, finite element.
[a]Hypothetical values to examine the effect of friction coefficient.

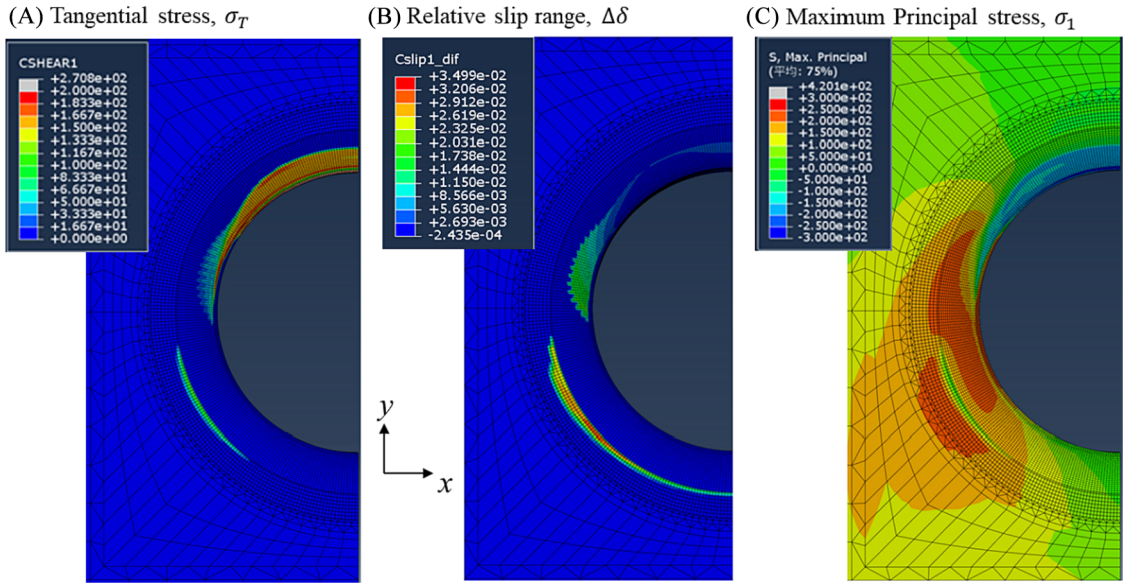

FIGURE 11 Distributions of (A) tangential stress (σ_T), (B) relative slip range ($\Delta\delta$), and (C) maximum principal stress (σ_1) at the contact surface of the Al alloy plate. [Colour figure can be viewed at wileyonlinelibrary.com]

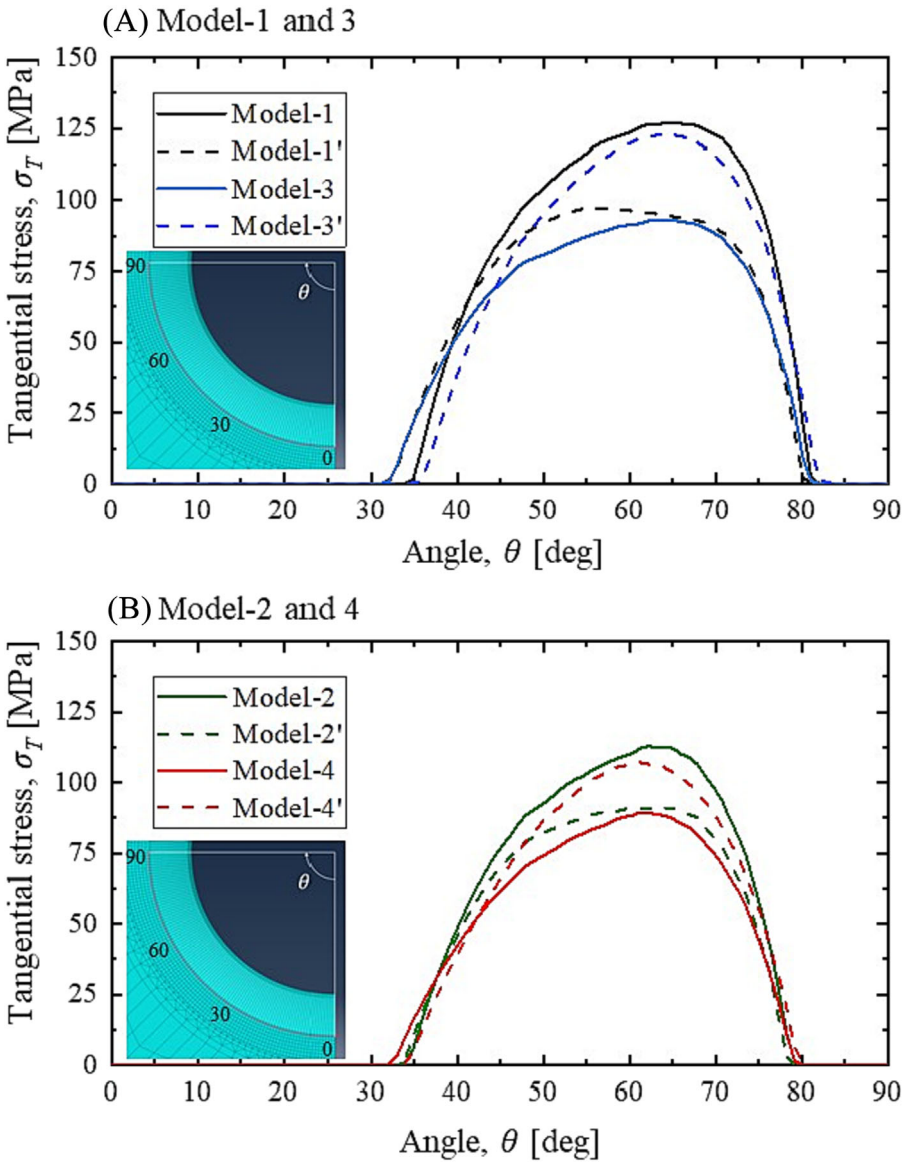

FIGURE 12 Tangential stress as a function of the angle from the bottom position. The computed values at the nodes along the red line in the insert are plotted for (A) Model-1 and Model-3 and (B) Model-2 and Model-4. [Colour figure can be viewed at wileyonlinelibrary.com]

5 | CONCLUSIONS

The fatigue strength of DSW dissimilar lap joints between steel sheets and Al alloys was investigated experimentally. Four types of DSW specimens were prepared using different combinations of steel sheets and aluminum alloys. These consisted of two types of steel sheets and two types of aluminum alloys. Tensile shear tests and fatigue tests were conducted at room temperature. A FE elastic plastic analysis was also performed to examine the stress along the contact surface of DSW specimens. The findings and conclusions of the investigations are as follows:

1. DSW specimens have tensile shear strengths equal to or greater than that of the SPR specimen. In DSW specimens fabricated with the lower-strength Al alloy, tensile fracture occurred in the Al alloy plate, whereas the tensile fracture occurred at the weld nugget in DSW specimens with the higher-strength Al alloy. The tensile shear strength of the latter DSW specimens was higher than that of the former.
2. The fatigue life of the DSW specimens was approximately 10 times longer than that of the SPR specimen. In all four DSW specimens, the fatigue crack initiated from the Al alloy associated with fretting induced by repeated contact and friction. Although the fatigue lives of the DSW specimens were mostly determined by the Al alloy strength, they were also affected by the steel sheet strength.
3. The tangential stress that caused fatigue damage and crack initiation was higher at a short distance away from the center hole of the Al alloy plate. This higher tangential stress area corresponded well to the actual site of crack initiation. Although the tangential stress was mostly governed by the friction coefficient, it was also affected by the steel sheet strength. The higher-strength steel led to the lower tangential stress, which resulted in the longer fatigue life of the DSW joint.

AUTHOR CONTRIBUTIONS

Motoki Sakaguchi: conceptualization, supervision, funding, writing–original draft, and writing–review and editing. **Yu Kurokawa**: formal analysis and writing–review and editing. **Fuminori Nakamura:** conducting experiment and methodology. **Toru HASHIMURA:** methodology and funding.

ACKNOWLEDGMENTS

Mark R. Kurban from Edanz (https://www.jp.edanz.com/ac) edited a draft of this paper.

CONFLICT OF INTEREST STATEMENT

The authors declare that they have no known competing financial interests or personal relationships that could have appeared to influence the work reported in this paper.

DATA AVAILABILITY STATEMENT

The data in this paper are available from the corresponding author upon reasonable request.

ORCID

Motoki Sakaguchi https://orcid.org/0000-0003-2862-4731

REFERENCES

1. Kuziak R, Kawakka R, Waengle S. Advanced high strength steels for automotive industry. *Arch Civ Mech Eng*. 2008;8(2):103-117.
2. Gullino A, Matteis P, D'Aiuto F. Review of aluminum-to-steel welding technologies for car-body applications. *Metals*. 2019;9(3):315.
3. Ma C, Chen DL, Bhole SD, Boundreau G, Lee A, Biro E. Microstructure and fracture characteristics of spot-welded DP600 steel. *Mater Sci Eng a*. 2008;485(1-2):334-346.
4. Brauser S, Pepke LA, Weber G, Rethmeier M. Deformation behavior of spot-welded high strength steels for automotive applications. *Mater Sci Eng a*. 2010;527(26):7099-7108.
5. Abe Y, Kato T, Mori K. Joinability of aluminium alloy and mild steel sheets by self-piercing rivet. *J Mater Process Technol*. 2006;177(1-3):417-421.
6. Hoang NH, Porcaro R, Langseth M, Hanssen AG. Self-piercing riveting connections using aluminium reviets. *Int J Solids Struct*. 2010;47(3-4):427-439.
7. Su ZM, Lin PC, Lai WJ, Pan J. Fatigue analyses of self-piercing rivets and clinch joints in lap-shear specimens of aluminum sheets. *Int J Fatigue*. 2015;72:53-65.
8. Porcaro R, Hanssen AG, Langseth M, Aalberg A. The behaviour of a self-piercing riveted connection under quasi-static loading conditions. *Int J Solids Struct*. 2006;43(17):5110-5131.
9. Sun X, Stephens EV, Khaleel MA. Fatigue behaviors of self-piercing rivets joining similar and dissimilar sheet metals. *Int J Fatigue*. 2007;29:307-386.
10. Huang L, Bonnen J, Lasecki J, Guo H, Su X. Fatigue and fretting of mixed metal self-piercing riveted joint. *Int J Fatigue*. 2016;83:230-239.
11. Hashimura T, Katsuma H, Iwaya J. New method for dissimilar metals joining of steel sheet and aluminum alloy using resistance spot welding and dimple shape, dimple spot welding (DSW). *Trans Soc Autom Eng Jpn*. 2017;48:1149-1154. (in Japanese)
12. Nakamura F, Sakaguchi M, Hashimura T. Fatigue properties of steel-aluminum alloy joint fabricated by dissimilar joining method DSW. *Trans Soc Autom Eng Jpn*. 2021;52(0):OS1107. (in Japanese).
13. Wagle S, Kato H. Ultrasonic detection of fretting fatigue damage at bolt joints of aluminum alloy plates. *Int J Fatigue*. 2009;31(8-9):1378-1385.
14. Nowell D, Dini D, Hills DA. Recent developments in the understanding of fretting fatigue. *Eng Fract Mech*. 2006;73(2):207-222.
15. Lykins CD, Mall S, Jain V. An evaluation of parameters for predicting fretting fatigue crack initiation. *Int J Fatigue*. 2000;22(8):703-716.
16. Bhatti NA, Wahab MA. Fretting fatigue crack nucleation: a review. *Tribol Int*. 2018;121:121-138.
17. Alfredsson B, Cadario A. A study on fretting friction evolution and fretting fatigue crack initiation for a spherical contact. *Int J Fatigue*. 2004;26(10):1037-1052.
18. Fatemi A, Socie DF. A critical plane approach to multiaxial fatigeu damage including out-of-phase loading. *Fatigue Fract Eng Mater Struct*. 1988;11(3):149-165.
19. Simith K, Topper T, Watson P. A stress-strain function for the fatigue of metals. *J Mater*. 1970;5:7.
20. Szolwinski MP, Farris TN. Mechanics of fretting fatigue crack. *Wear*. 198:93-107.
21. Liu KC. A method based on virtual strain-energy parameters for multiaxial fatigue life prediction. In: Mcdowell DL, Ellis R, eds. *Advances in Multiaxial Fatigue*. ASTM; 1993:67-84.
22. Lykins C, Mall S, Jain V. A shear stress-based parameter for fretting fatigue crack initiation. *Fatigue Fract Eng Mater Struct*. 2001;24(7):461-473.
23. Lykins C, Mall S, Jain V. Combined experimental-numerical investigation of fretting fatigue. *Int J Fatigue*. 2001;23(8):703-711.
24. Ruiz C, Boddington P, Chen K. An investigation of fatigue and fretting in a dovetail joint. *Exp Mech*. 1984;24(3):209-217.
25. Mutoh Y, Jayaparakash M. Tangential stress range-copressive stress range diagram for fretting fatigue design curve. *Tribol Int*. 44:1394-1399.
26. Nishioka K, Hirakawa K. Fundamental investigation of fretting fatigue, part 5, the effect of relative slip amplitude. *Bulletin of JSME*. 1969;12(52):692-697.
27. Mutoh Y. Mechanisms of fretting fatigue. *JSME Int*. 1995;38:405-415.

How to cite this article: Sakaguchi M, Kurokawa Y, Nakamura F, Hashimura T. Fatigue strength of steel–aluminum alloy dissimilar lap joints fabricated by dimple spot welding for automotive application. *Fatigue Fract Eng Mater Struct*. 2024;1-13. doi:10.1111/ffe.14227